

Extracting Symbolic Cycles from Turbulent Fluctuation Data

M. Lehrman and A. B. Rechester

Institute of Nonlinear Science Applications, 14 West St., Sharon, Massachusetts 02067

(Received 29 January 2001; published 27 September 2001)

The method for extracting symbolic cycles from the fluctuation data is presented. For the example of the Lorenz model we demonstrate that approximately the same complex structure of cycles can be computed using time records of different variables. Our method has been applied to the analysis of turbulent fluctuations measured in water flow in a pipe. Even though the fluctuations in the bulk of the water and near the wall of the pipe appear to be very different, the majority of the most stable cycles extracted from the data are identical.

DOI: 10.1103/PhysRevLett.87.164501

PACS numbers: 47.27.Eq, 05.40.-a, 05.45.-a, 47.11.+j

The purpose of this paper is to demonstrate how to extract from chaotic signals and turbulent fluctuation data the information related to the structure of unstable periodic orbits. There already exist algorithms for extracting periodic orbits from chaotic orbits for low-dimensional dynamical systems [1]. The advantage of our method is that it can be applied to the analysis of fluctuations measured experimentally in highly developed turbulence.

The Fourier transform is often used for the analysis of chaotic signals and turbulent fluctuations. It is useful for determining the coherent parts of fluctuating signals (which correspond to narrow peaks in the power spectrum) but it is not particularly informative for the analysis of the incoherent part of the signal (which corresponds to broad portions of the power spectrum). Consider the example of Fourier power spectra $F_x(\omega)$ and $F_z(\omega)$ presented in Fig. 1 [2,3]. Here signals $X(t)$ and $Z(t)$ are generated by the Lorenz model [2] and are related to fluid velocity and temperature fluctuations in a simplified model of Bénard thermal convection. $F_x(\omega)$ and $F_z(\omega)$ look quite different because the Fourier power spectrum is not an invariant characteristic of dynamics. On the other hand, the symbolic cycle distribution (SCD) introduced in this paper is approximately invariant [see Figs. 2(a) and 2(b)].

We will describe our method of computation for the example of the Lorenz model, and then apply it to the analysis of turbulent fluctuations measured experimentally in water flow in a pipe at Mason Laboratory, Yale University.

All computations below are defined for the $X(t)$ variable; exactly the same computations are done for the $Z(t)$ variable.

We begin with time discretization of our signals:

$$X_n = X(t_0 + n\tau). \tag{1}$$

Here $n = 0, 1, 2, \dots, N$. For the computations presented in Figs. 2(a) and 2(b), $\tau = 0.1$ and $N = 2 \times 10^5$. The criteria for choosing the appropriate τ and N are discussed below.

The time series X_n and Z_n are substituted by the symbolic series $S(X_n)$ and $S(Z_n)$. The symbolic dynamics used

for these computations is defined as

$$S(X_n) = \begin{cases} 0, & X_n - X_{n-1} \geq 0 \\ 1, & X_n - X_{n-1} < 0 \end{cases} \tag{2}$$

Such simple symbolic dynamics is adequate only for sufficiently small τ (see below).

The symbolic time series are partitioned into sequences of a given length L ($L = 7$ in the example below).

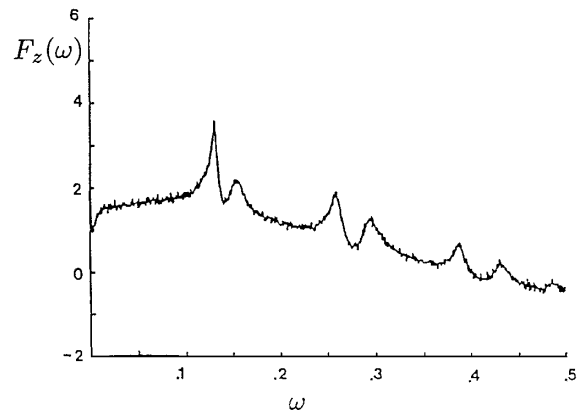
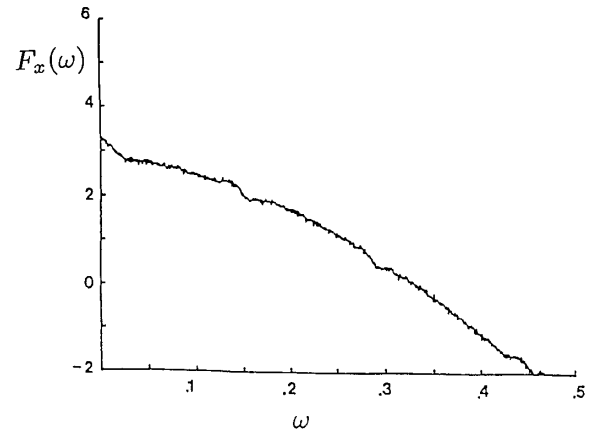
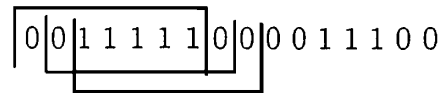


FIG. 1. Fourier power spectra $F_x(\omega)$ and $F_z(\omega)$ computed for $X(t)$ and $Z(t)$ signals generated from the Lorenz model.

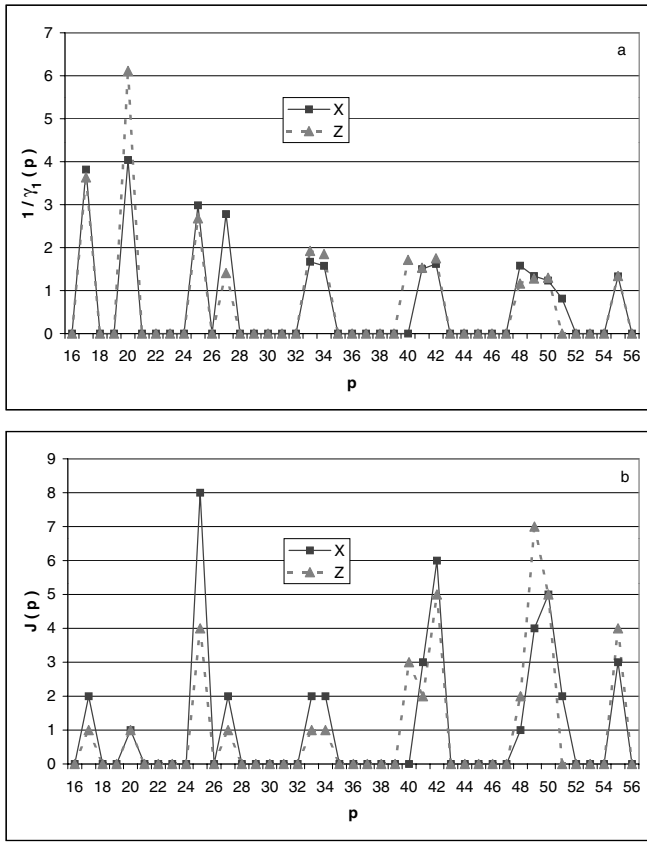


FIG. 2. (a) Stability parameter $1/\gamma_1(p)$ of the most stable cycles as a function of period computed for the signals $X(t)$ and $Z(t)$ for the Lorenz model: $a = 10$, $b = 8/3$, $r = 25$, $\tau = 0.1$, $L = 56$, and $N = 2 \times 10^5$. (b) Maximum number of cycles as a function of period $J(p)$ computed for the $X(t)$ and $Z(t)$ signals for the same parameters.

All sequences are identified uniquely by integers ℓ defined as

$$\ell(\{S_n\}_L) = \sum_{i=1}^L 2^{L-i} S_{n+i}. \quad (3)$$

Here we use the following notation for sequences of the length L , $\{S_n\}_L$: $S_{n+1}, S_{n+2}, \dots, S_{n+L}$.

We compute an information entropy defined as [4]

$$E(\tau, L, N) = - \sum_{\ell} P_{\ell} \ln P_{\ell}. \quad (4)$$

Here P_{ℓ} is the probability of finding a particular sequence ℓ , that is, the number of times N_{ℓ} this sequence is found in the symbolic time series, divided by the number of all sequences $(N - L) \approx N$. We find computationally that $E(\tau \rightarrow 0, L, N) \rightarrow 0$ and, in order to use symbolic dynamics with only two symbols as defined by Eq. (2), we need to choose τ small enough so that

$$E < L \ln 2. \quad (5)$$

Note that τ should not be too small because then we have to deal with very long periods (see below). We also found computationally that entropy is a monotonically increasing function of L and that $E(\tau, L \rightarrow \infty, N) \rightarrow \ln N$ and most

occupied “ ℓ ” states have $N_{\ell} = 1$. The symbolic kinetic equation, [(7) and (8)] based on a statistical description of dynamics, is valid if $N_{\ell} \gg 1$, thus L should be not too large so that

$$\exp E \ll N. \quad (6)$$

Relations between the probabilities P_{ℓ} are given by the symbolic kinetic equation [6]:

$$P_{\ell', n+1} = \sum_{\ell} P_{\ell, n} \Gamma(\ell \rightarrow \ell'), \quad (7)$$

$$\sum_{\ell'} \Gamma(\ell \rightarrow \ell') = 1. \quad (8)$$

Here $\Gamma(\ell \rightarrow \ell')$ is the probability of a transition from the state ℓ to the state ℓ' at one time step; it can be easily computed [6]. The sums in Eqs. (7) and (8) involve no more than two terms because we have only two symbols. The structure of the system of equations (7) and (8) can be represented graphically as a network diagram. A simple example of a network diagram is presented in Fig. 3 for $L = 6$ [6]. The numbers on this diagram correspond to the ℓ states while the arrows indicate the transitions between different states in one time step. This network diagram is taken from Ref. [6] just for the purpose of explaining the notion of symbolic cycles. Actual network diagrams which appear in our computations are so large that it is impossible to plot them.

Symbolic cycles which are related to unstable periodic orbits can be identified in the network diagram as closed loops. We will call the number of transitions or time shifts on the loop a period of the cycle “ p .” The simplest cycles correspond to the case $L = p$: in this case at every time shift a new symbolic state can be obtained from the old one by cyclic permutations of the sequence which defines the old symbolic state. For the example given in Fig. 3 there are two such cycles with $p = L = 6$. These cycles include the following transitions: (i) $29(011101) \rightarrow 58(111010) \rightarrow 53(110101) \rightarrow 43(101011) \rightarrow 23(010111) \rightarrow 46(101110) \rightarrow 29$. (ii) $59(111011) \rightarrow 55(110111) \rightarrow 47(101111) \rightarrow 31(011111) \rightarrow 62(111110) \rightarrow 61(111101) \rightarrow 59$. There are also many cycles with $p < L$. Consider

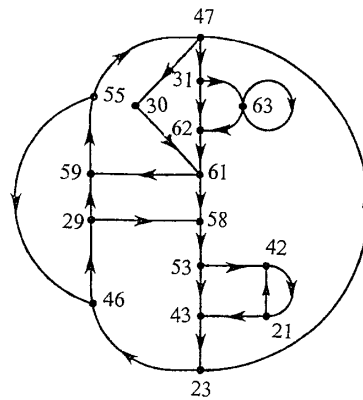


FIG. 3. Example of a network diagram for $L = 6$ [5].

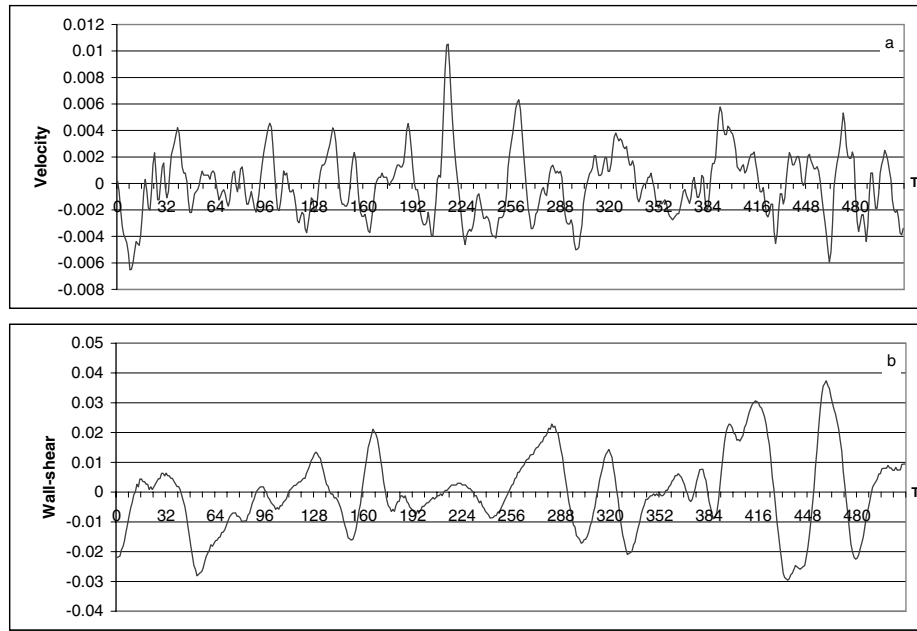


FIG. 4. Turbulent velocity fluctuations in the bulk of the water and wall shear simultaneously measured at the wall of the pipe [7].

first the case when $pm = L$; the permutation rules are still cyclic in this case. For the example given in Fig. 3 there are two such cycles with $p = 2$ [42(101010) \rightarrow 21(010101) \rightarrow 42] and another with period $p = 1$ [63(111111) \rightarrow 63]. For a more general case when L is not a multiple of p , we then have to cyclically permute every p th symbol counting from the end. For the example given in Fig. 3 there is a cycle of period $p = 5$ with the following transitions: 61(111101) \rightarrow 59(111011) \rightarrow 55(110111) \rightarrow 47(101111) \rightarrow 30(011110) \rightarrow 61. There is also a cycle of period $p = 4$ with the following transitions: 46(101110) \rightarrow 29(011101) \rightarrow 59(111011) \rightarrow 55(110111) \rightarrow 46. Cycles with $p > L$ will not be considered because the permutation rules for them could not be defined uniquely.

We can define the following stability parameter for a cycle:

$$\gamma_j(p) = -\frac{1}{p\tau} \sum_{i=1}^p \ln \Gamma\{\ell_j(i) \rightarrow \ell_j[\text{mod}_p(i+1)]\}. \quad (9)$$

Here the subscript $j = 1, 2, \dots, J(p)$ enumerates different cycles, while $\text{mod}_p(i+1) = 2, 3, \dots, p, 1$. Larger values of γ correspond to more unstable cycles. Do not confuse $\gamma_j(p)$ with Lyapunov numbers. If we consider the example of a stable periodic orbit, then the Lyapunov number is negative but the corresponding symbolic cycle will have $\gamma(p) \approx 0$. We order different cycles of the same period in the following way: $0 < \gamma_j < \gamma_{j+1}$, $\gamma_1 = \min \gamma_j(p)$.

Figure 2(a) plots the results of computations of the stability parameter $\gamma_1(p)$ for most stable cycles as a function of period p for the $X(t)$ and $Z(t)$ variables, which are not correlated in time. The points where $1/\gamma_1 = 0$ correspond to the periods for which cycles do not exist at all. We

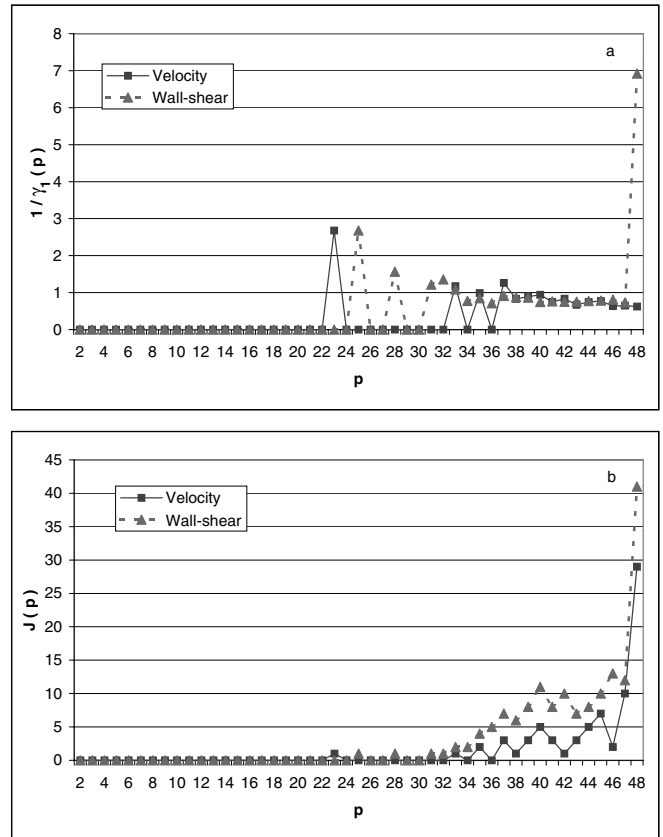


FIG. 5. (a) Stability parameter $1/\gamma_1(p)$ of the most stable cycles as a function of period computed for turbulent velocity and wall-shear fluctuations $\tau = 2 \times 10^{-4}$ sec, $L = 48$, and $N = 5 \times 10^5$. (b) Maximum number of cycles as a function of period $J(p)$ computed for the same signals; the parameters are the same.

chose $L = 56$ for this computation. The computations of the maximum number of cycles for the same period $J(p)$ are presented in Fig. 2(b). It is clear from these results that the symbolic cycle distribution is approximately invariant.

Now we present the application of our method for the analysis of turbulent fluctuations measured in water flow in a pipe [7].

The flow of water occurs in a pipe of 30 cm diameter, 30 m long, and the flow recirculates. The flow Reynolds number based on the pipe diameter is 300 000. The pipe is situated in Mason Laboratory at Yale University. Measurements were made by R. Bhiladvala [7]. One measurement was made at the pipe wall. This was a time signal of the shear stress fluctuation; one can show that this is the same as the velocity fluctuation very close to the wall. The other measurement was the velocity fluctuation away from the wall, right above the place where the shear stress was measured at the distance 3 cm above the wall stress probe. The time series for fluid velocity fluctuations and wall-shear simultaneously measured are presented in Fig. 4. The frequency of the digitizer was 10 kHz. There is practically no correlation between these two signals. These fluctuations look so different that one would assume that the nature of the turbulence at the wall and in the bulk of fluid is different. But the symbolic cycle distribution extracted from these data and presented in Figs. 5(a) and 5(b) shows that the majority of the most stable cycles are the same at the bulk of the water and at the wall. For these computations we used $\tau = 2 \times 10^{-4}$ sec, $L = 48$, and $N = 5 \times 10^5$.

The method presented in this paper was also applied to the analysis of turbulent plasma fluctuations measured in the tokamak. The results will be published elsewhere.

Thus we conclude that the method of SCD could be applied to the analysis of turbulence fluctuation data measured experimentally.

We are very thankful to Professor Edward N. Lorenz for comments, discussions, and encouragement and Professor Katepalli R. Sreenivasan (Yale University) and Dr. R. Bhiladvala (Yale University) for providing us with their turbulent fluctuation data. We are also very thankful to Dr. Robert Granetz, Dr. Earl Marmar, Dr. Todd Evans, and Dr. Roscoe White for useful discussions and comments. This work was partially supported by the U.S. Department of Energy under Contract No. DE-FG0291ER54130.

-
- [1] D. Auerbach, P. Cvitanovic, J. P. Eckmann, G. Gunaratue, and I. Procaccia, *Phys. Rev. Lett.* **58**, 2387 (1987).
 - [2] E. N. Lorenz, *J. Atmos. Sci.* **20**, 130 (1963).
 - [3] D. Farmer, J. Grutchfield, H. Froehling, N. Packard, and R. Shaw, *Ann. N.Y. Acad. Sci.* **357**, 453 (1980).
 - [4] C. E. Shannon and W. Weaver, *The Mathematical Theory of Communication* (University of Illinois Press, Urbana, IL, 1949).
 - [5] M. Lehrman, A. B. Rechester, and R. B. White, *Phys. Rev. Lett.* **78**, 54 (1997).
 - [6] A. B. Rechester and R. B. White, *Phys. Lett. A* **156**, 419 (1991).
 - [7] R. Bhiladvala, Ph.D. thesis, Yale University, 2000.